

# A time-frequency analysis of non-stationary signals using variation mode decomposition and synchrosqueezing techniques

Chao Ni, Tian Ran Lin\*, Jin Peng Xing, Jun Zhou Xue

Center for Structural Acoustics and Machine Fault Diagnosis,  
School of Mechanical and Automotive Engineering, Qingdao University of Technology  
Qingdao, China  
\*trlin@qut.edu.cn

**Abstract**—Time-frequency analysis (TFA) technique is an effective method in the analysis of non-stationary signals with multiple signal components. Nevertheless, the current TFA methods such as short-time Fourier transform (STFT) and synchrosqueezing transform (SST) suffer from low signal resolution and diffused energy problems in the processing of multi-component signals. To resolve such shortcoming, a new signal analysis technique utilizing a combined variational mode decomposition (VMD) and synchrosqueezing transform (SST) is proposed in this study. VMD is used first to decompose the signal into several intrinsic mode functions (IMFs). Kurtosis values of the IMFs are calculated to determine the fault sensitive components to be used in the signal reconstruction. The noise reduced reconstructed signal is then analyzed using SST to produce a clearer and energy concentrated time-frequency representation (TFR) for an improved bearing fault diagnosis. The validity of the presented technique is verified utilizing a computer simulated signal and a bearing defect signal acquired from the experiment.

**Keywords**—Synchrosqueezing transform; Variational mode decomposition; time-frequency reconstruction; kurtosis; Rényi entropy.

## I. INTRODUCTION

Rolling element bearings play a critical part in rotating machinery [1]. Its healthy condition directly affects the efficiency of a mechanical system. A change in bearing operating condition will lead to a change of the characteristics in the condition monitoring (CM) signal. Some bearing CM signals can even demonstrate nonlinearity and non-stationary characteristics due to a change of machine loading or speed conditions. TFA techniques are effective tools for the process of non-stationary signals which can capture the time-varying features of the signals. However, the conventional TFA methods such as short time Fourier transform (STFT) and wavelet transform analysis (WT) have certain limitations in dealing with strong time-varying signals. For example, STFT uses a fixed sliding time window in the transform, the frequency and time domains cannot achieve good resolution due to Heisenberg uncertainty principle. WT can effectively overcome the shortcoming of STFT though the mother wavelet function used in the transform needs to be selected manually, selecting a wrong mother wavelet function can lead to different analysis results.

A series of novel signal post-processing techniques have recently been presented aiming to solve such problem. Daubechies et al. [2] presented a synchrosqueezing (SST) technique and binding it with wavelet transform (SWT) in a time frequency analysis. Thakur et al. [3] proposed an alternative synchrosqueezing technique based on STFT to define the

instantaneous frequencies (IF) of a multi-component amplitude-modulated-frequency-modulated (AM-FM) signal. The later approach has been successfully employed in many fields including mechanical fault diagnosis [4] and earthquake analysis [5]. However, the performance of SST is sensitive to noise interference, which can lead to an inaccurate TFR of a signal. An iterative generalized SST was proposed by Feng et al. [6] to tackle the diffused TFR energy problem of a multi-component non-stationary signal. The technique is then applied for fault diagnosis of a planetary gearbox. Other post-processing techniques such as demodulation SST [7] and synchroextracting transform (SET) [8] have also been proposed to address the diffused TFR energy problem of SST.

In dealing with noise contaminated signals, Qin et al. [9] used a combined Empirical Mode Decomposition (EMD) [10] and SST technique to reduce the influence of noise for an improved time-frequency resolution. However, EMD has the well-known mode mixing and end effect problems which can cause problems in its application. Dragomiretskiy et al. [11] presented an alternative adaptive technique namely variational mode decomposition (VMD) to resolve the end effect and mode mixing problems of EMD. VMD is utilized in this paper which is used alongside SST to achieve an accurate time frequency analysis and for signal reconstruction. In this approach, a noise contaminated fault signal is decomposed and denoised using VMD, the kurtosis of each mode from VMD analysis is calculated and the two modes having the highest kurtosis values are retained to be used in SST. Finally, the TFRs from SST analysis are added for the signal reconstruction of the fault signal containing multiple defect signal components.

The remaining of the paper is arranged as follows: In Section II, the theory knowledge of SST, VMD and kurtosis are briefly introduced. The combined time frequency analysis technique based on VMD and SST as well as the signal analysis procedure are elaborated in Section III. The validity of the proposed method is verified utilizing a computer simulated speed varying signal in Section IV, and a compound bearing defect signal from the experiment in Section V. Conclusions are drawn in Section VI.

## II. THEORETICAL BACKGROUND

### A. SST based on STFT

In this section, the theoretical background of SST analysis based on STFT is introduced. SST can squeeze the scattered TF energy of STFT into the IF trajectory position. A single

The financial support from the Shandong Provincial Government key research project grant (Grant No 2018GGX109011) for this work is gratefully acknowledged

component signal  $x(t) = Ae^{j2\pi f_0 t}$  is used in the following analysis to exemplify the principle of the technique.

The STFT of signal  $x(t)$  can be expressed as [8]:

$$G(t, \omega) = \int_{-\infty}^{+\infty} x(u)g(u-t)e^{-j\omega u} du \quad (1)$$

where  $g(u-t)$  denotes the sliding time window function.

To simplify the mathematical expression, let  $g_\omega(u) = g(u-t)e^{j\omega u}$ , in terms of Parseval's theorem, Eq. (1) expression is described below:

$$\begin{aligned} G(t, \omega) &= \int_{-\infty}^{+\infty} x(u) \cdot (g(u-t)e^{j\omega u})^* du = \\ &= \int_{-\infty}^{+\infty} x(u) \cdot (g_\omega(u))^* du = \\ &= \frac{1}{2\pi} \int_{-\infty}^{+\infty} \bar{x}(\xi) (\bar{g}_\omega(\xi))^* d\xi \end{aligned} \quad (2)$$

where  $()^*$  denotes the conjugate operation,  $\bar{g}_\omega(\xi)$  denotes the Fourier transform of the  $g_\omega(u)$  and  $\bar{x}(\xi)$  is the Fourier transform of  $x(u)$  where the overhead bar represents the Fourier transform.

Letting  $t' = u - t$ ,  $\bar{g}_\omega(\xi)$  can be obtained as:

$$\begin{aligned} \bar{g}_\omega(\xi) &= \int_{-\infty}^{+\infty} g(t') e^{j\omega(t+t')} e^{-j\xi(t+t')} dt' \\ &= e^{j(\omega t - \xi t)} \int_{-\infty}^{+\infty} g(t') e^{j(\omega - \xi)t'} dt' \\ &= \bar{g}(\omega - \xi) e^{j(\omega t - \xi t)} \end{aligned} \quad (3)$$

Substituting Eq. (3) into Eq. (2) and adding the phase shift operator  $\exp(j\omega t)$ , the improved STFT is given by

$$G_e(t, \omega) = \frac{1}{2\pi} \int_{-\infty}^{+\infty} \bar{x}(\xi) \cdot \bar{g}(\omega - \xi) e^{j\xi t} d\xi \quad (4)$$

The FT of the signal  $x(t)$  can be computed by:

$$\bar{x}(\xi) = 2\pi A \cdot \delta(\xi - 2\pi f_0) \quad (5)$$

Substituting Eq. (5) into Eq. (4), the STFT of signal  $x(t)$  can now be written as:

$$G_e(t, \omega) = A \bar{g}(\omega - 2\pi f_0) e^{j2\pi f_0 t} \quad (6)$$

According to Eq. (6), the time-frequency energy of the signal will spread in the frequency interval  $[2\pi f_0 - \Delta, 2\pi f_0 + \Delta]$  where  $\Delta$  is the frequency support of the sliding time window function.

To calculate the instantaneous frequency of the signal, we can take the partial derivative of STFT regard to time as:

$$\begin{aligned} \partial_t G_e(t, \omega) &= \partial_t (A \bar{g}(\omega - 2\pi f_0) e^{j2\pi f_0 t}) \\ &= j2\pi f_0 A \bar{g}(\omega - 2\pi f_0) e^{j2\pi f_0 t} = j2\pi f_0 G_e(t, \omega) \end{aligned} \quad (7)$$

where  $G_e(t, \omega) \neq 0$ , the estimated instantaneous frequency  $f_0$  can then be obtained by:

$$f_0(t, \omega) = -j \frac{\partial_t G_e(t, \omega)}{2\pi G_e(t, \omega)} \quad (8)$$

Once the instantaneous frequency is estimated, SST can be performed to gather the time frequency coefficients along the instantaneous frequency trajectory, which is formulated as:

$$SST(t, \omega) = \int_{-\infty}^{+\infty} G_e(t, \omega) \delta(\omega - f_0(t, \omega)) d\omega \quad (9)$$

where  $\int_{-\infty}^{+\infty} \delta(\omega - f_0(t, \omega)) d\omega$  is the synchrosqueezing operator and  $\delta$  denotes the Dirac delta function.

SST can enhance the energy concentration of the TFR of a weak time varying signal. However, the energy distribution of SST can diffuse heavily along the instantaneous trajectory for multi-component and for strong speed varying signals.

### B. Variational mode decomposition

VMD is a novel signal decomposition technique [11]. VMD can adaptively decompose a multi-component signal into the righteous signal components. Unlike that of EMD, VMD defines the intrinsic mode function (IMF) as AM-FM signals:

$$u_k(t) = A_k(t) \cos(\phi_k(t)) \quad (10)$$

where  $u_k$  denotes the  $k$ th IMF,  $A_k$  is the amplitude, and  $\phi_k$  is the phase of the component,  $A_k(t) \geq 0$ ,  $\phi'_k(t) \geq 0$ .

Taking the Hilbert transform on each mode to obtain an analytic signal component as follows:

$$\tilde{u}_k(t) = (\delta(t) + \frac{j}{\pi t}) * u_k(t) \quad (11)$$

The mode  $u_k$  corresponding to the estimated center frequency  $e^{-j\omega_k t}$  can be extracted according to:

$$\widehat{u}_k(t) = \tilde{u}_k(t) e^{-j\omega_k t} \quad (12)$$

The bandwidth of the extracted mode  $\widehat{u}_k$  is estimated by calculating the squared  $L^2$ -norm of the demodulated signal. The constrained variational problems can be constructed as follows:

$$L^2_{\text{norm}} = \arg \left\{ \min_{\{u_k\}, \{\omega_k\}} \left\{ \sum_k \|\partial_t \widehat{u}_k(t)\|_2^2 \right\} \right\} \quad (13)$$

$$\text{subject to } \sum_k u_k(t) = x(t) \quad (14)$$

where  $\{u_k\}$  denotes the ensemble of the variational modes  $\{u_1, u_2, \dots, u_k\}$ ,  $\{\omega_k\}$  represents a series of center frequencies corresponding to  $\{u_k\}$ .  $x(t)$  represents the input signal.

To settle the constraint variational problem, the quadratic penalty term and the Lagrange multiplier are utilized. The augmented Lagrangian expression is given as follows:

$$L(\{u_k\}, \{\omega_k\}, \lambda) = \alpha \sum_k \|\partial_t \hat{u}_k(t)\|_2^2 + \left\| x(t) - \sum_k u_k(t) \right\| + \langle \lambda(t), x(t) - \sum_k u_k(t) \rangle \quad (15)$$

where  $\alpha$  denotes the quadratic penalty term,  $\lambda(t)$  is the Lagrange multiplier.

The alternate direction method of multipliers (ADMM) can be used to iteratively settle the variational problem. The modal component  $u_k^{n+1}$  and the frequency  $\omega_k^{n+1}$  can be obtained from:

$$u_k^{n+1}(t) = iFFT \left\{ \frac{\hat{x}(\omega) - \sum_{k \neq K} u_k(\omega) + \frac{\lambda(\omega)}{2}}{1 + 2\alpha(\omega - \omega_k)^2} \right\} \quad (16)$$

where  $iFFT$  represents inverse fast Fourier transform, and

$$\omega_k^{n+1} = \frac{\int_0^\infty \omega |u_k(\omega)|^2 d\omega}{\int_0^\infty |u_k(\omega)|^2 d\omega} \quad (17)$$

### C. Kurtosis

Kurtosis is a parameter to describe the impulse peaks in a waveform which is rather sensitive to impact signals [12]. For a discrete signal  $x(t)$ , the kurtosis is defined as follows:

$$K = \frac{E(x - \mu)^4}{\sigma^4} \quad (18)$$

where  $E(x - \mu)^4$  denotes the fourth order expectation,  $\mu$  represents the mean value of the signal, and  $\sigma$  represents the standard deviation.

When the bearing is operated at the normal condition, the amplitude distribution of the condition monitoring signal is close to a normal distribution where the kurtosis value is minimum [15]. Following the occurrence and development of a bearing fault, the signal amplitude distribution would deviate from the normal distribution leading to the increase of the kurtosis value. Thus, the kurtosis value can be used to determine the IMF components to be kept for the signal reconstruction to produce a noise reduced signal to be used in SST analysis.

### III. THE PROCEDURES OF THE PROPOSED SIGNAL ANALYSIS TECHNIQUE

The signal analysis procedures of the method are demonstrated as follows:

- (1) Decomposes the original signal into several IMFs ( $u_k(t)$ ) using VMD
- (2) Calculates the kurtosis value of each IMF
- (3) Selects the relevant IMFs having the smallest and the largest

kurtosis values are superimposed for signal reconstruction to reduce the noise contamination and to prevent the information loss

- (4) Employs SST for the time frequency analysis of the reconstructed signal

$$SST_{u_k}(t, \omega) = \int_{-\infty}^{+\infty} G_{u_k}(t, \omega) \delta(\omega - f_{u_k}(t, \omega)) d\omega \quad (19)$$

### IV. ANALYSIS OF A COMPUTER SIMULATED SIGNAL

In this section, the validity of the presented method is evaluated on a simulated variable speed bearing fault signal based on that of Ref. [13]. The signal components of the defect signal are given as follows:

$$\begin{aligned} s_1(t) &= \sin(8000\pi t) (15t + 10\cos(30(\cos(\frac{\pi}{3}t)))) \\ s_2(t) &= \sum_{m=1}^M A_m \exp\{-0.15[t - t_m]\} \sin\{4.8\pi f_r[t - t_m]\} \mu[t - t_m] \\ s(t) &= s_1(t) + s_2(t) \end{aligned} \quad (20)$$

where  $M$  denotes signal length,  $A_m$  is the amplitude envelop of the  $m^{th}$  impulse,  $t_m$  is the occurrence time of impulse,  $\mu(t)$  is a unit step function, and the simulated bearing defect frequency is  $2.4f_r$ . The sampling frequency is 12 kHz and the sampling number is 12k respectively. The shaft rotating frequency ( $f_r$ ) varies from 15 Hz to 24 Hz within the 1 s interval. The simulated waveform is shown in Fig. 1.

The decomposed IMFs of the simulated signal using VMD are demonstrated in Fig. 2. The kurtosis value of each IMF is displayed in Table I. It is observed that IMF2 and IMF3 have the minimum and the maximum kurtosis values respectively. As a result, these two components are superimposed to restructured the noise reduced signal to be used in the subsequent SST analysis. The TFR of the reconstructed signal using SST is shown in Fig. 3(a). It is shown that the proposed technique can clear capture the TFRs of the defect components with relatively high energy concentration along the instantaneous frequency (IF) trajectories. For comparison, the TFRs of the original signal from the SST and STFT analysis are exhibited in Figs. 3(b) and 3(c). It is shown that the defect signal energies are diffused along the IF trajectories if only SST is used in the analysis without the VMD processing step. Whilst the signal energy from STFT analysis is rather blurry in the time frequency plane which can hinder an accurate machine fault diagnosis.

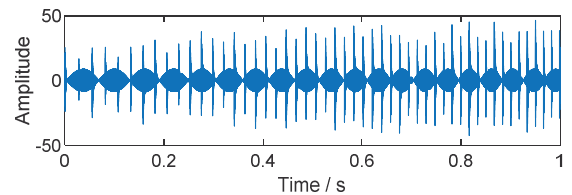


Fig. 1 The time waveform of the simulated signal

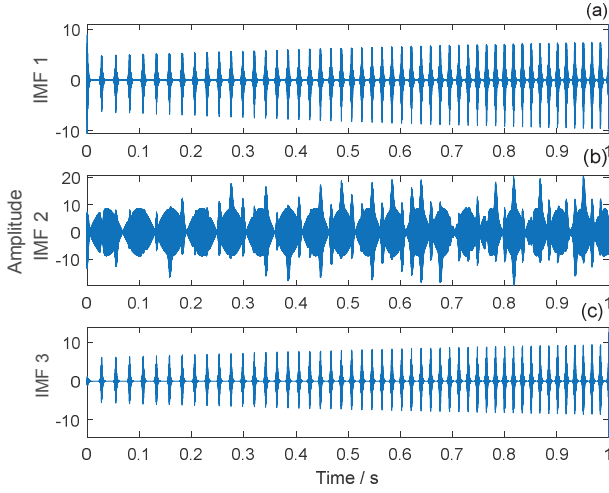


Fig. 2 The IMFs of the signal from VDM decomposition

TABLE I The kurtosis values of the IMFs from VDM decomposition

IMF	1	2	3
Kurtosis Value	10.4016	2.9777	13.2068

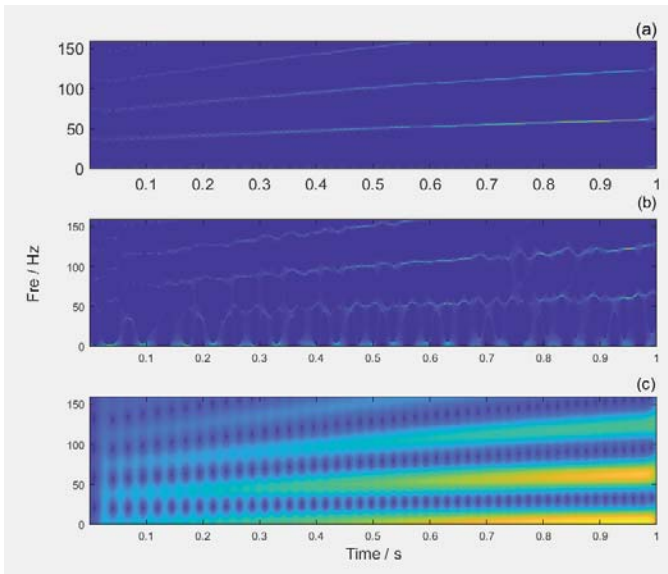


Fig. 3 (a) The proposed technique, (b) SST, (c) STFT.

Rényi entropy is a commonly used indicator to quantitatively evaluate the energy concentration level of TFR results, the smaller Rényi entropy denotes the more energy-concentrated TFR. The Rényi entropies for the three time-frequency analysis techniques are shown in Table II. It is shown that the Rényi entropy value calculated from the TFR result of the current approach is the smallest, which indicates that the proposed technique is superior than the other two TF techniques in the analysis of the speed varying defect signal.

TABLE II Rényi entropy of each TFA

	STFT	SST	Current technique
Rényi entropy	21.4242	19.5964	16.2674

## V. ANALYSIS OF AN EXPERIMENTAL DATA

In this section, a bearing defect signal acquired from a Spectra Quest's Machinery Fault Simulator as shown in Fig. 4 is used to validate the validity of the presented method. The test bearing used in the experiment has a compound fault including the outer race fault, the inner race fault and a defect rolling element. The specific parameters of the bearing are shown in Table III. The vibration signal is acquired by B&K4370 accelerometer which was placed on the top of the bearing house. The sampling frequency is set at 10 kHz, and the sampling length is 0.4 s. The shaft rotation speed is set at 1260 rpm (i.e., a rotation frequency  $f_r = 21$  Hz). The corresponding bearing defect frequencies can be calculated as follows:

$$\text{Inner ring: } f_i = 5.43f_r$$

$$\text{Outer ring: } f_o = 2.322f_r \quad (21)$$

$$\text{Rolling element: } f_b = 2.322f_r$$

The time waveform of the vibration condition monitoring (CM) data acquired from the experiment is shown in Fig. 5(a), and the IMFs of the signal decomposed using VMD is demonstrated in Fig. 5(b). The kurtosis value of each IMF is displayed in Table VI. It is demonstrated that IMF1 and IMF3 have the minimum and the maximum kurtosis values respectively. These two IMFs are then superimposed to form a reconstructed noise reduced signal to be used in the subsequent SST analysis.

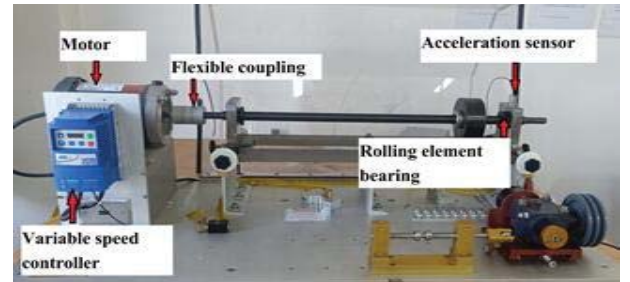


Fig. 4 Spectra Quest's Machinery Fault Simulator

TABLE III Type ER-16K roller element bearing and its parameters

Parameter	Value
Inner ring diameter (mm)	25.4
Pitch diameter (mm)	38.5064
Rolling element (mm)	37.9375
Number of rolling element (n)	9
Contact angle (°)	9.08



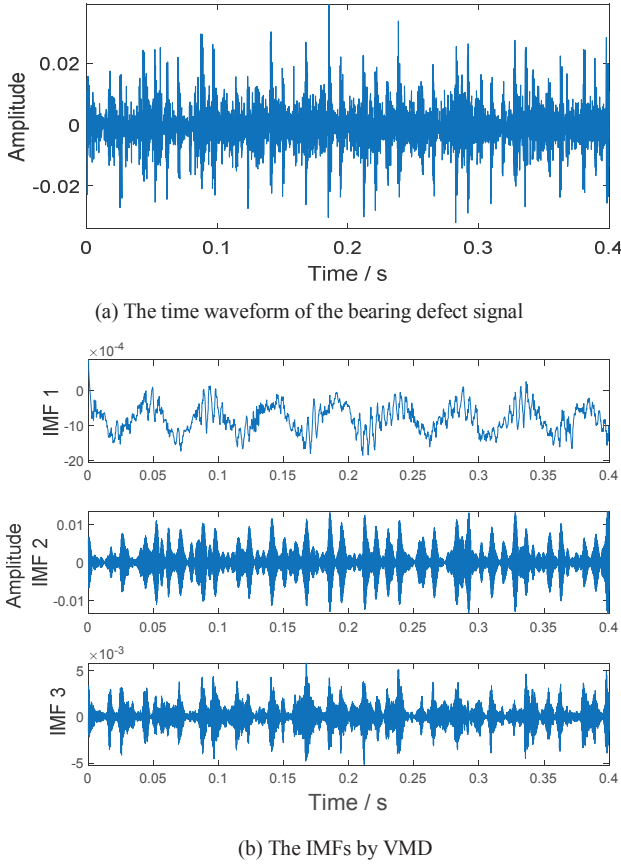


Fig. 5 (a) The original signal, and (b) IMFs from VMD decomposition

TABLE VI Calculated kurtosis values of IMFs

IMF	1	2	3
Kurtosis	2.9497	4.7714	4.9255

The TFR of the reconstructed signal from the SST analysis is demonstrated in Fig. 6(a). All the three bearing defected frequency components are clearly shown in the time frequency domain. In contrast, the defect information contained in the TFRs obtained from a direct SST and STFT analysis of the original signal are either less clear or completely lost as demonstrated in Figs. 6(b) and 6(c).

The Rényi entropies of the TFRs shown in Fig. 6 are displayed in Table IV. Similar to the simulated signal, the Rényi entropy of the TFR analyzed utilizing the presented method is the lowest within the three.

TABLE V The Rényi entropy values of the TFRs

Method	STFT	SST	Current technique
Rényi entropy	21.8853	20.4796	18.4911

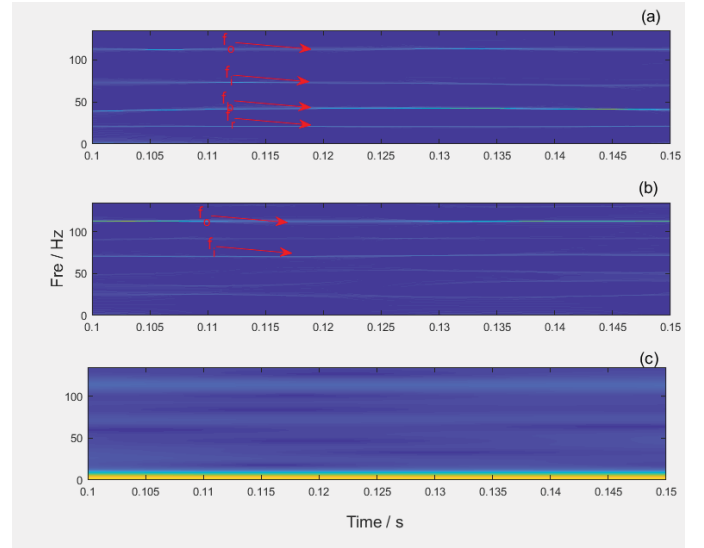


Fig. 6 Time frequency analysis using (a) Current approach, (b) SST, (c) STFT.

## VI. CONCLUSION

A time frequency analysis method combining VMD and SST techniques was proposed in this paper for an improved bearing fault diagnosis. The validity of the presented method was verified by using a computer simulated speed varying signal and a compound bearing defect signal acquired from a bearing test rig. The performance of the proposed technique is also evaluated by comparing the results obtained using the proposed technique and those obtained using SST and STFT analysis. It is found that the proposed technique can outperform the other two time-frequency analysis techniques by producing an energy concentrated TFRs in the time frequency plane for an accurate bearing fault diagnosis.

## REFERENCES

- [1] T. R. Lin, E. Kim, and A. C. C. Tan . "A practical signal processing approach for condition monitoring of low speed machinery using Peak-Hold-Down-Sample algorithm." *Mechanical Systems and Signal Processing* . vol.36, no.2, pp. 256-270, 2013.
- [2] I. Daubechies, J. F. Lu, and H.-T. Wu, "Synchrosqueezed wavelet transform: An empirical mode decomposition like tool," *Appl. Comput. Harmon. Anal.* vol. 30, no. 2, pp. 243-261, Mar. 2011.
- [3] G. Thakur, H. T. Wu. "Synchrosqueezing-Based Recovery of Instantaneous Frequency from Nonuniform Samples." *SIAM Journal on Mathematical Analysis*. vol.43, no.5 , pp.2078-2095, 2011.
- [4] C. Li, L. Ming. "Time-frequency signal analysis for gearbox fault diagnosis using a generalized synchrosqueezing transform." *Mechanical Systems and Signal Processing* . vol. 26, pp. 205-217, July 2011.
- [5] R. H. Herrera, M. van der Baan, and J. Han. "Applications of the synchrosqueezing transform in seismic time-frequency analysis." *Geophysics*. vol.79, no.3, pp.55-64, 2014.
- [6] D. H. Pham, and S. Meignen. "High-Order Synchrosqueezing Transform for Multicomponent Signals Analysis—With an Application to Gravitational-Wave Signal." *IEEE Transactions on Signal Processing*. vol. 65 no. 12, pp. 3168-3178, 2017.
- [7] X. T. Tu, Y. Hu, F. C. Li, S. Abbsa, Z. Liu, and W. J. Bao. "Demodulated High-Order Synchrosqueezing Transform with Application to Machine Fault Diagnosis." *IEEE Transactions on Industrial Electronics*. vol.66, no.4, pp. 3071-3081, 2019.
- [8] G. Yu, M. Yu, and C. Xu. "Synchroextracting Transform." *IEEE Transactions on Industrial Electronics* . vol.64, no.10, pp. 8042-8054, 2017.

- [9] X. Qin, et al. "Microseismic data denoising method based on EMD mutual information entropy and synchrosqueezing transform." *Geophysical Prospecting for Petroleum*. vol.56, no.5, pp. 658-666, 2017.
- [10] N. E. Huang, et al. "The empirical mode decomposition and the Hilbert spectrum for nonlinear and non-stationary time series analysis." *Proceedings: Mathematical, Physical and Engineering Sciences*. vol.454, no.1971, pp. 903-995, 1998.
- [11] K. Dragomiretskiy, and D. Zosso. "Variational Mode Decomposition." *IEEE Transactions on Signal Processing*. vol.62, no.3, pp. 531-544, 2014.
- [12] R. B. Randall. "Vibration-based condition monitoring: industrial, aerospace and automotive applications." A John Wiley and Sons, Ltd., Publication. Dec 19, 2010.
- [13] G. Yu. "A Concentrated Time Frequency Analysis Tool for Bearing Fault Diagnosis." *IEEE Transactions on Industrial Electronics and Measurement*. pp.1-11, March 2019.